International Journal of Nanomedicine

Dovepress
open access to scientific and medical research

Open Access Full Text Article

ORIGINAL RESEARCH

Tumor Microenvironmental Responsive Liposomes Simultaneously Encapsulating Biological and Chemotherapeutic Drugs for Enhancing Antitumor Efficacy of NSCLC

This article was published in the following Dove Press journal:
International Journal of Nanomedicine

Liang Kong[1]
Shi-meng Zhang[2]
Jia-hao Chu[3]
Xin-ze Liu[1]
Lu Zhang[1]
Si-yu He[1]
Si-min Yang[3]
Rui-jun Ju[3]
Xue-tao Li[1]

[1]School of Pharmacy, Liaoning University of Traditional Chinese Medicine, Dalian 116600, People's Republic of China; [2]Department of Neurology, Linyi People's Hospital, Linyi 276003, People's Republic of China; [3]Department of Pharmaceutical Engineering, Beijing Institute of Petrochemical Technology, Beijing 102617, People's Republic of China

Background: Non-small cell lung cancer (NSCLC) is one of the most lethal types of cancer with highly infiltrating. Chemotherapy is far from satisfactory, vasculogenic mimicry (VM) and angiogenesis results in invasion, migration and relapse.

Purpose: The objective of this study was to construct a novel CPP $_{(mmp)}$ modified vinorelbine and dioscin liposomes by two new functional materials, DSPE-PEG_{2000}-MAL and CPP-PVGLIG-PEG_{5000}, to destroy VM channels, angiogenesis, EMT and inhibit invasion and migration.

Methods and Results: The targeting liposomes could be enriched in tumor sites through passive targeting, and the positively charged CPP was exposed and enhanced active targeting via electrostatic adsorption after being hydrolyzed by MMP2 enzymes overexpressed in the tumor microenvironment. We found that CPP $_{(mmp)}$ modified vinorelbine and dioscin liposomes with the ideal physicochemical properties and exhibited enhanced cellular uptake. In vitro and in vivo results showed that CPP $_{(mmp)}$ modified vinorelbine and dioscin liposomes could inhibit migration and invasion of A549 cells, destroy VM channels formation and angiogenesis, and block the EMT process. Pharmacodynamic studies showed that the targeting liposomes had obvious accumulations in tumor sites and magnificent antitumor efficiency.

Conclusion: CPP $_{(mmp)}$ modified vinorelbine plus dioscin liposomes could provide a new strategy for NSCLC.

Keywords: vinorelbine, dioscin, non-small cell lung cancer, multi-functional liposomes, tumor microenvironment, MMP2 enzymes

Correspondence: Xue-tao Li
School of Pharmacy, Liaoning University of Traditional Chinese Medicine, Shengming 1 Road 77, Double D Port, Dalian 116600, People's Republic of China
Tel +86411 8589 0170
Fax +86411 8589 0128
Email lixuetao1979@163.com

Rui-jun Ju
Department of Pharmaceutical Engineering, Beijing Institute of Petrochemical Technology, Qingyuan North Road 19, Beijing 102617, People's Republic of China
Tel +8610 8129 2387
Fax +8610 8129 2124
Email juruijun@bipt.edu.cn

Introduction

Lung cancer can be categorized into non-small-cell lung cancer (NSCLC) and small-cell lung cancer (SCLC) according to pathological classification. About 85% of all lung cancers are NSCLC, and their morbidity and mortality are still rising rapidly worldwide.[1] Although conventional therapeutics have achieved modest improvements, it is frustrating that the 5-year survival rate for NSCLC patients is still only 14–16%. In fact, cancer-related deaths always occur because of distant metastasis mainly caused by the migration and invasion of tumor cells, which indicates that the spread of primary tumor cells to distant places is the main obstacle to successful treatment of NSCLC.[2] Therefore, the development of new

treatments to inhibit the migration and invasion of cancer cells has become an important topic in the fight against NSCLC.

Invasion and migration occur through a multi-step process, and approximately 90% of cancer deaths arise from the invasive and metastatic spread. Usually, tumor cells shift through the vasculature, stagnate in distant capillaries, penetrate into surrounding tissues, and eventually spread into distant organs into tumors.[3] In order to prevent NSCLC metastasis to prolong the survival of patients, several approaches have been proposed, such as traditional Chinese medicine therapy, the development of new compounds, chemo-immunotherapy, etc.[4–6] Among them, the chemo-immunotherapy combinations will become the first-line treatment for NSCLC, which significantly improved the progression-free survival (PFS) and overall survival (OS) rates of these patients. First-line chemo-immunotherapy combinations are starting to and will certainly revolutionize the current paradigm of metastatic NSCLC treatment because of their superior performance in PFS and OS, compared to the based chemotherapy.[7] However, there are problems with these associations, and the chemo-immunotherapy combinations will obviously lead to an increase in treatment-related toxicity and a higher discontinuation rate. Therefore, these treatments should be administered carefully.[8] In recent years, the rapid development of nanotechnology has shown unprecedented effects in the treatment of NSCLC and prevention of metastasis by enhancing the permeability and retention (EPR) effects of primary tumors or metastatic sites.[9]

As a nanoscale drug carrier, liposomes are promising drug encapsulation system that can encapsulate hydrophilic and hydrophobic drugs. Liposomes have many advantages, including targeting capability, long-term efficacy, improved drug stability, reduced drug toxicity, and increased circulation time.[10] However, conventional liposomes are easily swallowed by the RES system in vivo and lose their active targeting effect. In order to improve the stability of liposomes in vivo, it is usually necessary to modify some hydrophilic groups on the liposomal surface.[11] However, the close contact between liposomes and tumor cells was greatly hindered by the hydrophilic modification, thereby reducing the active targeting to tumor cells. Therefore, it is an urgent problem to ensure the stability of liposomes and improve the active targeting of liposomes in vivo.[12] Conventional targeted liposomes could only passively accumulate near leaky site of tumor vessels, but they cannot reach the deep region of tumor. To further improve the tumor penetration efficiency, we developed a novel strategy of co-administering cell-penetration peptides with size-shrinkable and tumor-microenvironment-responsive multistage system to overcome these barriers. In response to the differences in physiological internal environment and tumor microenvironment in vivo, targeted liposomes can change their physical and chemical properties to achieve deeper tumor penetration, enhance cell uptake and timely release of drugs.

As we knew that tumor microenvironment plays a key role in tumor proliferation, invasion and metastasis, including hypoxia, acidic pH, high pressure, and abnormal expression of related cytokines and inflammatory response, etc.[13,14] Based on extensive research on tumor microenvironment and drug targeting, there is still room for further improvement, "dual" and even "multi-functional" drug carriers have been proposed and developed.[15] Matrix metalloproteases (MMPs) contain a family of zinc-dependent secreted endopeptidases that are of interest due to their ability to degrade extracellular matrices (ECMs). It is reported that MMP2 and MMP2 enzymes are frequently overexpressed in the majority of solid tumors, such as NSCLC, breast cancer, colon cancer, and its important role in promoting cancer progression makes it a significant target for tumor therapy.[16–18] On the basis of these findings, we designed an enzymatically cleavable targeting molecule whose hydrophilic long-chain PEG_{5000} can be enzymatically removed in a tumor microenvironment with high expression of MMP2 enzymes.

In this study, we designed and developed a novel multi-functional liposome that responds to overexpressed MMP2 enzymes, resulting in the enhanced tumor targeting and internalization. In our design, the MMP2-cleavable peptide (Pro-Val-Gly-Leu-Ile) was used as a sensitive linker between a liposomal lipid and its long-chain PEG block, acting as a steric barriers for the nanoparticle and surface-attached cell-penetrating peptide (CPP) in the blood. When being exposed to tumor microenvironment, the peptide is cleaved by the highly expressed extracellular MMP2 enzymes, leading to the exposure of CPP for enhancing intracellular penetration. In addition, vinorelbine and dioscin were encapsulated into the liposomes as a cytotoxic drug and a regulator that inhibited tumor metastasis, neovascularization, and VM channels formation, respectively (Figure 1). We expect microenvironmental responsive multifunctional targeted liposomes can provide an

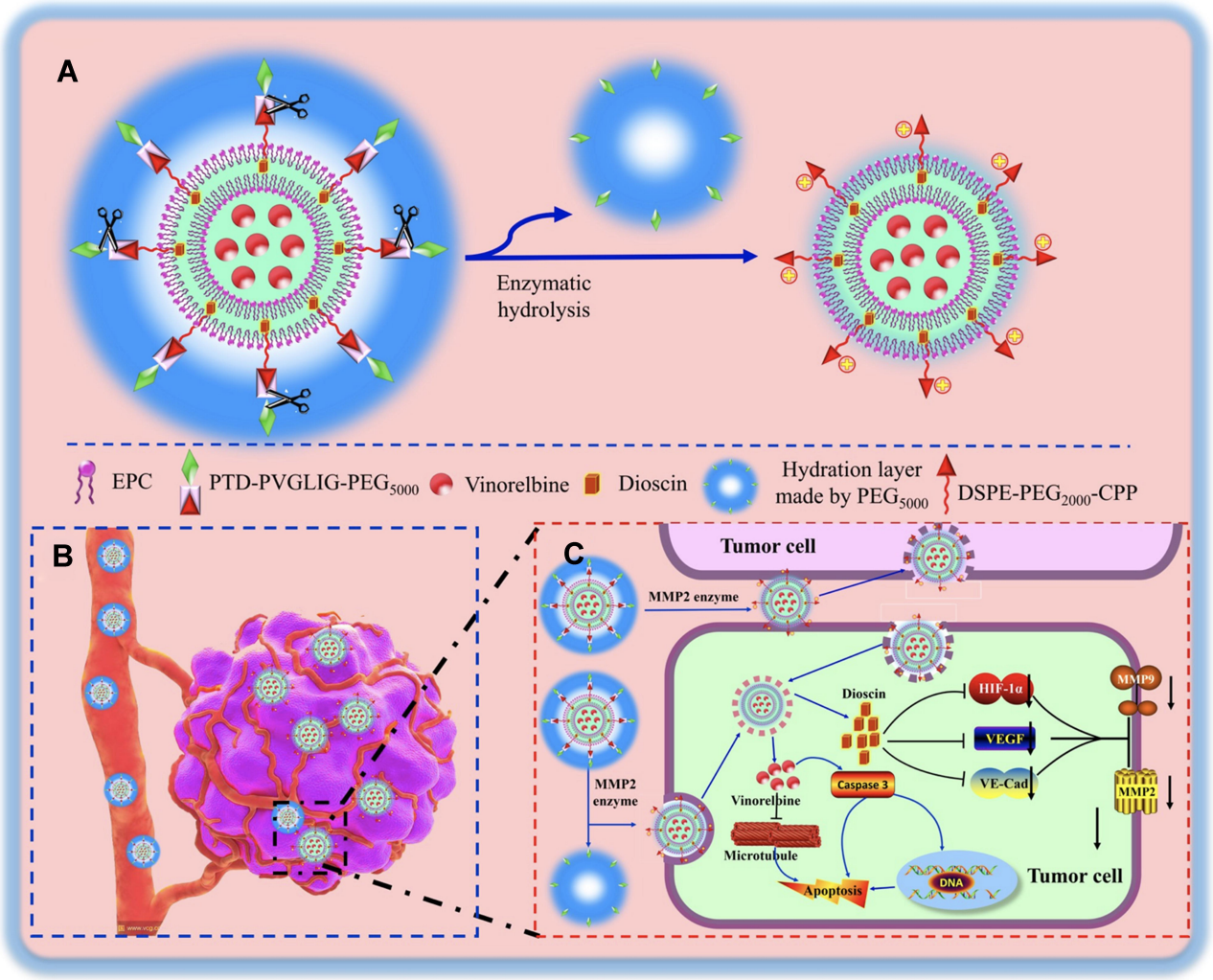

Figure 1 Schematic illustration of strategy for treating NSCLC by CPP $_{(mmp)}$ modified vinorelbine plus dioscin liposomes. (**A**) A schematic representation of enzymatic hydrolysis of CPP $_{(mmp)}$ modified vinorelbine plus dioscin liposomes. (**B**) The enhanced transport drug carrier to tumors and enzymatic hydrolysis to expose CPP. (**C**) Anti-apoptosis and the inhibition of VM channels formation mediated by vinorelbine and dioscin, respectively.

innovative strategy for the treatment and facilitate the clinical treatment of NSCLC.

Materials and Methods

Materials and Cells

Egg yolk phosphatidylcholine (EPC), cholesterol (Chol), and 1.2-distearoyl-sn-glycero-3-phosphoethanolamine-N [carboxy (polyethylene glycol)-2000] (DSPE-PEG_{2000}-MAL) were purchased from the Avanti Polar Lipids, Inc. (Alabaster, AL, USA). Polyethylene glycol-distearoyl phosphatidylethanolamine (DSPE-PEG_{2000}) was obtained from the NOF Corporation (Tokyo, Japan). Vinorelbine, hematoxylin and eosin (HE) staining kit, alcian blue periodic acid schiff (AB-PAS) stain kit and terminal deoxynucleotidyl transferase-mediated dUTP-biotin nick end labeling (TUNEL) kit were obtained from the Meilun Biotechnology Co., Ltd. (Dalian, China). Dioscin was supplied by the Chengdu Derick Biotechnology Co., Ltd. (Chengdu, China). mPEG_{5000}-PVGLIG-RKKRRQRRRC (CPP-PVGLIG-PEG_{5000}) was synthesized by the GL Biochem Co., Ltd. (Shanghai, China). Ki67, CD-31 antibody and HRP-labelled secondary antibody were ordered from Biosynthesis Biotechnology Co., Ltd. (Beijing, China). 4′, 6-diamidino −2-phenylindole (DAPI) and 1.1-dioctadecyl-3,3,3,3- tetramethylindotricarbocyanine iodide (DiR) were supplied by Kaiji Biological Technology Development Co., Ltd. (Nanjing, China).

Human NSCLC A549 cells were purchased from the Institute of Basic Medical Science, Chinese Academy of Medical Science (Beijing, China). Cells were cultured in RPMI-1640 culture medium supplemented with 10% fetal

bovine serum (FBS) (EallBio, Beijing, China), 100 U/mL penicillin and 100 μg/mL streptomycin at 37°C in a humidified atmosphere of 95% air and 5% CO_2. Male BALB/c nude mice of 20 ± 2 g were obtained from the Peking University Experimental Animal Center (Beijing, China). This research was approved by the Institutional Authority for Laboratory Animal Care of Peking University. The guidelines followed for animal welfare were based on the Interim Measures for the Control of Experimental Animals of Peking University No. 166 [2010].

Synthesis of DSPE-PEG_{2000}-CPP-PVGLI-PEG_{5000}

At pH 6.8, the maleimide group of DSPE-PEG_{2000}-MAL efficiently reacted with the sulfhydryl group of CPP-PVGLI-PEG_{5000} peptide (1:1, a molar ratio), and then adjusted pH of the reaction solution to 9.0 with N-methylmorpholine. The reaction solution was stirred overnight at room temperature (RT), and dialyzed overnight (MWCO. 8000 Da) to remove unbound material. Subsequently, the solution was lyophilized and stored at −20°C. Then, it was characterized by matrix-assisted laser desorption/ionization time-of-flight mass spectrometry (MALDI-TOF-MS, Shimadzu, Japan).

Preparation of Liposomes

MMP2-responsive liposomes were prepared using thin-film hydration according to a previous method.[19] In short, EPC, Chol, DSPE-PEG_{2000}, DSPE-PEG_{2000}-CPP-PVGLI-PEG_{5000}, and dioscin were dissolved in methyl alcohol at a molar ratio of 100:30:1:1:5 in a pear-shaped bottle, dried by rotary evaporator at 37°C to obtain a thin film, and the thin film was hydrated with 5 mL ammonium sulfate by sonication in a water bath. The suspensions were then sonicated in an ice bath with a probe sonicator for 10 minutes at 200 W. Subsequently, the samples were extruded through the polycarbonate membranes for 3 times with 200 nm pores. Then, the above liposomes were transferred to a cellulose ester membrane (MWCO 1.2–1.4 kDa) for dialysis 3 times with PBS. After dialysis, vinorelbine was encapsulated (EPC: vinorelbine = 1000:1, molar ratio) in a water bath at 40°C with shaking for 20 min, thus preparing CPP $_{(mmp)}$ modified vinorelbine plus dioscin liposomes. All the other liposomes were prepared as above, and the raw materials are shown in Table 1. In order to measure the distribution of liposomes in vitro and in vivo, epirubicin and DiR were entrapped into liposomes to replace vinorelbine, the lipids/epirubicin and lipids/DiR were set at 20:1 and 200:1 (w/w), respectively.

Table 1 The Composition of the Varying Liposomal Formulations

	Raw Materials	Molar Ratio
Blank control liposomes	EPC: Chol: DSPE-PEG_{2000}	100:30:1
Vinorelbine liposomes	EPC: Chol: DSPE-PEG_{2000}: vinorelbine	100:30:1:0.1
Dioscin liposomes	EPC: Chol: DSPE-PEG_{2000}: dioscin	100:30:1:5
Vinorelbine plus dioscin liposomes	EPC: Chol: DSPE-PEG_{2000}: vinorelbine: dioscin	100:30:1:0.1:5
CPP $_{(mmp)}$ modified vinorelbine plus dioscin liposomes	EPC: Chol: DSPE-PEG_{2000}: DSPE-PEG_{2000}-CPP-PVGLI-PEG_{5000}: vinorelbine: dioscin	100:30:1:1:0.1:5

Enzymatic Hydrolysis of Targeting Molecule and Targeting Liposomes

The lyophilized DSPE-PEG_{2000}-CPP-PVGLIG-PEG_{5000} was dissolved in distilled water, and quantitative MMP2 enzymes were subsequently added with a mole ratio of 1:1. Then the solution was gently stirred at room temperature for 2 h. After being dialyzed 3 times with PBS solution (MWCO. 5000 Da), the PBS solution was lyophilized and characterized by MALDI-TOF-MS.[20] In order to elaborate the degradation process of CPP $_{(mmp)}$ modified vinorelbine plus dioscin liposomes, the changes of physicochemical properties were measured after the addition of MMP2 enzymes. In brief, 4 mL CPP $_{(mmp)}$ modified vinorelbine plus dioscin liposomes and 1 mL MMP2 enzymes were simultaneously added into a centrifuge tube; then, the tube was continuously shaken at 37°C for 2 h. Then, particle size, polydispersity index (PDI) and zeta potential of CPP $_{(mmp)}$ modified vinorelbine plus dioscin liposomes before and after addition of MMP2 enzymes were measured by a Nano Series Zen 4003 Zetasizer (Malvern Instruments Ltd., Malvern, UK). Both vinorelbine and dioscin contents were measured using a high-performance liquid chromatography system (HPLC) with an ultraviolet detector (Shimadzu LC-2010AHT) and the un-encapsulated drugs were separated by elution against a Sephadex G-50 column. The encapsulation efficiencies (EE) were calculated using the following equation: EE %=($W_{encapsulated\ drug}/W_{total\ drug}$) ×100%.[21] The morphology of CPP $_{(mmp)}$ modified

vinorelbine plus dioscin liposomes was examined by a transmission electron microscopy (TEM, JEM-1200EX; JEOL, Tokyo, Japan) and an atomic force microscopy (Cypher AFM, Asylum Research Inc, Santa Barbara, CA, USA).

Cellular Uptake and Distribution

A549 cells were seed (2×10^5 cells) in 6-well plates and cultured for 24 h at 37°C. Epirubicin was entrapped into liposomes and used as the fluorescent probe for observing the cellular uptake and distribution.[22] The varying formulations were added at an equivalent epirubicin concentration of 10 μM, the cells were incubated in culture medium for 2 h and cells treated with CPP $_{(mmp)}$ modified epirubicin plus dioscin liposomes were added with different concentrations of MMP2 enzyme (0.2 μM for L, 0.5 μM for M, and 1 μM for H) and incubated for 2 h. The culture medium was used as blank control. Then, cells were washed with PBS, harvested by trypsinization and centrifuged at 1500 rpm for 3 min. The precipitate was resuspended in 300 μL PBS and the samples were quantitative evaluated by a flow cytometry (BD Biosciences, Franklin Lakes, NJ).

Fluorescence confocal microscope was used to further observe the cellular uptake of the varying formulations in A549 cells. The cells were incubated with the varying formulations at 10 μM concentration of epirubicin for 2 h, the medium was removed and cells were washed with PBS, fixed with 4% paraformaldehyde in PBS for 15 min at RT, and then the nuclei of cells were counterstained with DAPI for 10 min. Finally, the cellular uptake and distribution were analyzed by a fluorescence confocal microscope (Nikon Cl-si TE2000, Tokyo, Japan).[19,23]

Destructing Effects in A549 Cells Spheroids

In order to evaluate the destructing effects of CPP $_{(mmp)}$ modified vinorelbine plus dioscin liposomes on the spheroids, A549 spheroids were prepared according to our previous reports.[24] After culturing for 48 h, A549 cell spheroids were collected into 6-well plates, and then treated with the varying formulations at a concentration of 0.2 μM vinorelbine. Blank control was treated with culture medium. After 48 h of incubation, the spheroids were fixed by 2.5% glutaraldehyde for 60 min, washed with cold PBS, dehydrated and embedded. The spheroids were observed under a scanning electron microscope (SEM, JSM-5600 LV, JEOL, Japan).

Cytotoxicity Assay

A549 cells were seed into 96-well plates (1.5×10^4 cells) and cultured for 24 h, the culture medium was replaced with fresh culture media containing varying concentrations of free vinorelbine, free dioscin, and free vinorelbine plus dioscin for the free drugs treatment groups, respectively. The concentration of vinorelbine ranged from 0 to 0.1 μM. In liposomal groups, the cells were treated with blank liposomes and the varying drug-loaded liposomes. The concentration range of vinorelbine was 0 to 0.2 μM. After incubation for 48 h, cell viability was determined by Cell Counting Kit-8 (CCK-8) assay based on measurement of absorbance at 540 nm using a microplate reader (HBS-1096A, DeTie, Nanjing, China). The survival rate was calculated using the following equation: survival %= $(A_{540\ nm\ for\ treated\ cells}/A_{540\ nm\ for\ untreated\ cells})\times100\%$. Finally, dose–effect curves were plotted according to the assay data. The half inhibitory concentration of cells (IC_{50}) was calculated, and each assay was repeated in triplicate.[23,25]

VM Channel Formation Assay

A Matrigel-based tube formation assay was used to assess the activity of the varying liposomes against the VM channels of A549 cells. Matrigel was added into a 96-well plate (50 μL/well) and incubated at 37°C for 30 min until solidified. A549 cells (4×10^4 cells) were resuspended with serum-free medium containing the varying liposomal formulations (the concentration of 0.2 μM vinorelbine and 10 μM dioscin), and culture medium was used as blank control. After incubation for 5 h, VM channels were observed and photographed using an inverted microscope (Nikon Eclipse E800, Nikon, Tokyo).[26]

Angiogenesis Assay in Chick Chorioallantoic Membranes

To establish the experimental model of chick chorioallantoic membranes (CAM), fertilized hen eggs were selected. Eggs were sterilized and incubated for 7 days at 37°C, a window was opened on the fertilized egg shell to expose the CAM, and the window was closed with sterile tape. The eggs were sequentially cultured at 37°C for 24 h. Then, sterile silicone rings were placed on the vascular-rich site, and the varying liposomal formulations

were added to the silicone ring at a final concentration of 0.2 μM vinorelbine and 10μM dioscin, and the windows were then closed.[27] After 48 h of incubation, the CAM was captured with a digital camera and the blood vessel area was analyzed using image pro plus 5.0 software.

Cell Migration Assay

A549 cells' migration was evaluated using a Transwell assay. Briefly, A549 cells suspended in 100 μL serum-free media were seeded into the upper compartment of each chamber of a 24-well plate. FBS-containing medium (600 μL) was added into the lower chambers. Then, the cells in upper chamber were treated with varying liposomal formulations at a final concentration of 0.2 μM vinorelbine and 10μM dioscin. After incubation for 24 h, cells in the upper chambers were removed with a cotton swab, and the invasive cells in the lower chambers were fixed with 4% paraformaldehyde for 15 min, and stained using a 0.5% crystal violet solution or 30 min and were then counted under a microscope. This experiment was performed in triplicate.

Wound-Healing Assay

A549 cells were seeded into 6-well plates and cultured at 37°C until 90% confluent. Then, cells were scratched with a 20 μL sterile pipette tip to create a wound that was run along the dish bottom. The plates were washed 3 times to remove cell debris and then the varying liposomal formulations were added into the medium at a final concentration of 0.2 μM vinorelbine and 10μM dioscin. The cells were observed at different time points (0 and 24 h) and the wound closure was determined by a microscope. Each experiment was performed in triplicate. Calculation formula of wound-healing rate: wound-healing rate (%) = (wound area $_{0\ h}$- wound area $_{24\ h}$)/wound area $_{0\ h}$× 100%.[28]

Epithelial–Mesenchymal Transition

The inhibitory effect of epithelial-mesenchymal transition (EMT) was evaluated by cell heating analysis. A549 cells were seeded (7×10^5) in a 6-well plate for 24 h, and then the cells were treated with the varying formulations for 6 h at final concentration of 0.2 μM vinorelbine and 10μM dioscin. The cells were then washed 3 times with PBS and trypsinized. After suspension with the medium, the cells were bathed at 47°C for 10 min, and then re-cultured in a 6-well plate for 12 h. The blank control group received no treatment. The cells were observed and photographed under a microscope. The ratio of EMT in cells was calculated by the following formula: EMT ratio (%) = NS/NN × 100%, where "NS" represents the number of spindle cells in a random field of view, and "NN" is the number of normal A549 cells in a random field of view.[29]

In vivo Imaging and Specificity to Tumor Sites in Tumor-Bearing Mice

BALB/c nude mice bearing subcutaneous A549 xenograft tumors were used for liposomal targeting evaluation. Tumor-bearing mice models were prepared according to our previous reports. DiR-loaded liposomes (2 μg DiR each mouse) were injected into these model mice via tail vein. Subsequently, the mice were anesthetized with isoflurane, and fluorescent images and X-ray images of the mice were captured at 1, 2, 6, 12, 24, and 48 h using an in vivo fluorescence imaging system (Carestream, FX Pro, USA). The mice were sacrificed at 48 h, the tumor masses, hearts, livers, spleens, lungs, and kidneys were dissected for ex vivo fluorescence imaging.

Antitumor Efficacy in vivo

To evaluate the antitumor effects of the varying drug formulations in vivo, lung cancer cell xenograft mice model was established. When the average tumor volume reached about 70 mm^3, the mice were randomly divided into 5 groups (8 mice per group), and the varying drug formulations (7.5 mg/kg dioscin and 0.4 mg/kg vinorelbine), and saline were injected into mice via tail vein at day 14, 16, 18 and 20. Body weights and tumor volumes were monitored every 2 days, Tumor volume was measured using the formula: tumor volume = 0.5 ($a \times b^2$), where "a" and "b" refer to the largest and smallest diameter, respectively. Mice were sacrificed on the 24th day, tumors were isolated, and paraffin sections were prepared for HE staining, TUNEL and immunocytochemistry analysis.

Statistical Analysis

All data were expressed as the mean ± SD and were analyzed using GraphPad Prism 6.0. Differences between groups were assessed by one-way ANOVA. Individual *t*-test was used for comparison between the two groups. $P < 0.05$ was considered statistically significant.

Results and Discussion

The incorporation of responsive moieties into the targeted drug delivery systems may achieve precise targeting

ability and controlled release of drug, thereby improving their therapeutic effect and reducing toxicity. The altered production of certain extracellular proteins in the tumor microenvironment may be important for tumorigenesis and development.[30] MMPs, especially MMP2 and MMP9, are involved in the invasion and metastasis of most human tumors due to the degradation of surrounding connective extracellular matrix (ECM). It is reported that MMP2 and MMP2 enzymes are highly expressed in most solid tumors, including NSCLC, breast cancer, colorectal cancer, liver cancer, prostate cancer, pancreatic cancer and ovarian cancer, etc.[31,32] Herein, the extracellular MMP2 enzymes sensitive bond (PVGLI) is used as a stimulus to trigger the enhanced tumor targeting in our newly designed nano-liposomes.

Characterization and Enzymatic Hydrolysis of the Targeting Molecules

We characterized the targeting molecules using MALDI-TOF-MS, and results are shown in Figure 2A–C. The average masses of DSPE-PEG_{2000}-MAL and DSPE-PEG_{2000}-CPP-PVGLIG-PEG_{5000} were 3018.66 (Figure 2A) and 9705.34 (Figure 2B), respectively. According to the MALDI-TOF-MS spectrum, the mass difference between the molecules of DSPE-PEG_{2000}-MAL and DSPE-PEG_{2000}-CPP-PVGLIG-PEG_{5000} corresponded to the mass of the CPP-PVGLIG-PEG_{5000} peptide, confirming the successful synthesis of the targeting molecules. When DSPE-PEG_{2000}-CPP-PVGLIG-PEG_{5000} was incubated with MMP2 enzymes for 2 h, the average mass was changed to 4168.86 (Figure 2C). Compared with DSPE-PEG_{2000}-CPP-PVGLIG-PEG_{5000}, and the mass difference was mainly due to the leaving of hydrophilic group of PEG_{5000} hydrolyzed by MMP2 enzymes, thus exposing the positively charged CPP to enhance the active targeting via electrostatic adsorption.

Characterization and Enzymatic Hydrolysis of the Targeting Liposomes

Characteristics of CPP $_{(mmp)}$ modified vinorelbine plus dioscin liposomes can be observed in Figure 2D–F. TEM (Figure 2D) and AFM (Figure 2E and F) images showed that CPP $_{(mmp)}$ modified vinorelbine plus dioscin liposomes had a smooth surface, and approximately 100 nm in diameter with a narrow size distribution (≤0.20). The particle size of liposomes is an important factor for their physical and biological properties, such as stability, cellular uptake pathway, and metabolism in vivo.[33] In this study, results suggested that the mean particle size of CPP $_{(mmp)}$ modified vinorelbine plus dioscin liposomes was 107.64±8.96 nm (Figure 2G), which was in accordance with the TEM observations. However, after treatment with MMP2 enzymes, the hydrophilic group of PEG_{5000} was liberated from the liposomal surface due to the cleavage of MMP2-cleavable linker, and the particle size was shrunk to about 87.86±5.53 nm (Figure 2H). It was reported that the size-shrinkable ability of nanocarriers could lead to tumor deep penetration.[34] The zeta potential value of CPP $_{(mmp)}$ modified vinorelbine plus dioscin liposomes was close to neutral state (Figure 2I), and the positively charged CPP was exposed to the liposomal surface, causing an obvious increase of the zeta potential value after the addition of MMP2 enzymes (Figure 2J). Hence, the modification of CPP-PVGLIG-PEG_{5000} on the liposomal surface could improve physical stability in vivo, avoid the clearance by RES, prolong circulation time, and enhance the active targeting. In addition, both drugs could be successfully loaded into liposomes with high entrapment efficiencies (EE%) of above 90% (Table 2).

Cellular Uptake and Targeting Effects in vitro

To study cell penetration ability of CPP $_{(mmp)}$ modified vinorelbine plus dioscin liposomes, cellular uptake and targeting effects were carried out. However, because of vinorelbine and dioscin have no fluorescence characteristics, we selected epirubicin with fluorescence as the fluorescent probe to evaluate the cellular uptake of liposomes.[22] A549 cells were used for NSCLC therapy researches in this study. In Figure 3, quantitative evaluation by flow cytometry showed that the order of fluorescence intensity was in the following sequence: free epirubicin > CPP $_{(mmp)}$ modified epirubicin plus dioscin liposomes +MMP2 enzymes > epirubicin liposomes ≥ epirubicin plus dioscin liposomes > CPP $_{(mmp)}$ modified epirubicin plus dioscin liposomes (Figure 3A and B). We found that when free epirubicin was administered, it had the highest uptake for direct drug-cell contact. For liposomal formulations, the particle size of liposomes (approximately 100 nm) blocked the intracellular uptake by A549 cells. Compared with epirubicin plus dioscin liposomes, CPP $_{(mmp)}$ modified epirubicin plus dioscin liposomes showed little fluorescence signal in tumor

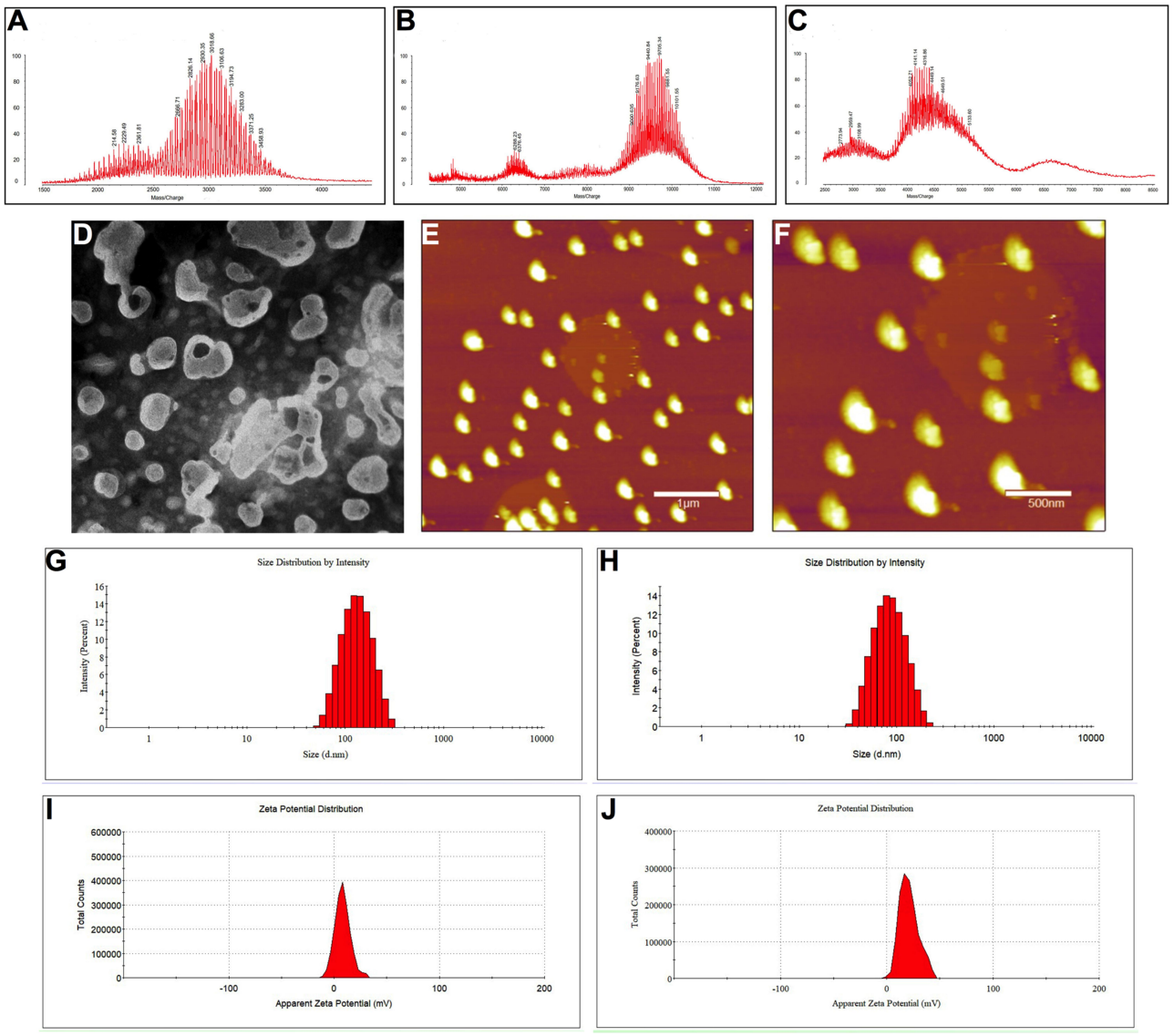

Figure 2 Characterization of CPP $_{(mmp)}$ modified vinorelbine plus dioscin liposomes. (**A**) MALDI-TOF-MS spectrum of DSPE-PEG$_{2000}$-MAL; (**B**) MALDI-TOF-MS spectrum of DSPE-PEG$_{2000}$-CPP-PVGLIG-PEG$_{5000}$; (**C**) MALDI-TOF-MS spectrum of DSPE-PEG$_{2000}$-CPP; (**D**) TEM image of CPP $_{(mmp)}$ modified vinorelbine plus dioscin liposomes, scalar bar=100 nm; (**E**) AFM image of CPP $_{(mmp)}$ modified vinorelbine plus dioscin liposomes, scale bar=1 μm; (**F**) the amplified structure of (**E**), scale bar=500 nm; (**G**) particle size of CPP $_{(mmp)}$ modified vinorelbine plus dioscin liposomes; (**H**) particle size of CPP $_{(mmp)}$ modified vinorelbine plus dioscin liposomes incubated with MMP-2 enzymes; (**I**) Zeta potential of CPP $_{(mmp)}$ modified vinorelbine plus dioscin liposomes; (**J**) Zeta potential of CPP $_{(mmp)}$ modified vinorelbine plus dioscin liposomes incubated with MMP-2 enzymes.

cells for the protection of hydrophilic group of PEG$_{5000}$. When such formulations were incubated with MMP2 enzymes, the cleavable linker of PVGLI was degraded and the blockage of PEG$_{5000}$ on the liposomal surface was eliminated. The exposed positively charged CPP significantly enhanced the intracellular uptake by A549 cells via electrostatic adsorption. Therefore, there are two key functions in the targeting delivery system, one is PEG-mediated CPP shielding effect which can minimize non-specific uptake, and the other is MMP2 enzyme sensitivity which can increase the penetration of antitumor drugs in tumor microenvironment with over-expressed MMP2 enzyme activity.

As shown in Figure 3C and D, it was revealed that cellular uptake of fluorescent probe slightly enhanced after CPP $_{(mmp)}$ modified epirubicin plus dioscin liposomes were treated with the increasing concentration of MMP2 enzymes. Furthermore, in order to more clearly observe the liposome localization in the A549 cells, laser scanning confocal microscopy was used. A strong fluorescence signal could be observed in the cellular membrane and the nuclei of A549 cells after incubation with CPP $_{(mmp)}$ modified epirubicin

Table 2 Characterization of All the Liposomes

	Encapsulation Efficiency (%)		Particle Size (nm)	PDI	Zeta Potential (mV)
	Vinorelbine	Dioscin			
Vinorelbine liposomes	93.65±4.65	—	88.37±2.65	0.19±0.01	1.63±0.15
Dioscin liposomes	—	90.64±5.42	90.66±3.65	0.20±0.02	2.75±0.55
Vinorelbine plus dioscin liposomes	97.64±5.32	91.37±2.53	92.64±7.32	0.19±0.01	2.32±0.53
CPP $_{(mmp)}$ modified vinorelbine plus dioscin liposomes	94.72±6.31	90.43±5.64	107.64±8.96	0.19±0.02	6.31±0.35
CPP $_{(mmp)}$ modified vinorelbine plus dioscin liposomes + MMP2 enzymes	93.72±6.52	92.54±3.65	87.86±5.53	0.17±0.01	17.54±0.43

plus dioscin liposomes + MMP2 enzymes (Figure 3E). Figure 3F represents the destructive effects on A549 spheroids. Results showed that the tightly organized spheroids became disintegrated and shrunken after treatment with CPP $_{(mmp)}$ modified vinorelbine plus dioscin liposomes + MMP2 enzymes. For the varying liposomal formulations, the rank of destructive effects on the spheroids was CPP $_{(mmp)}$ modified vinorelbine plus dioscin liposomes + MMP2

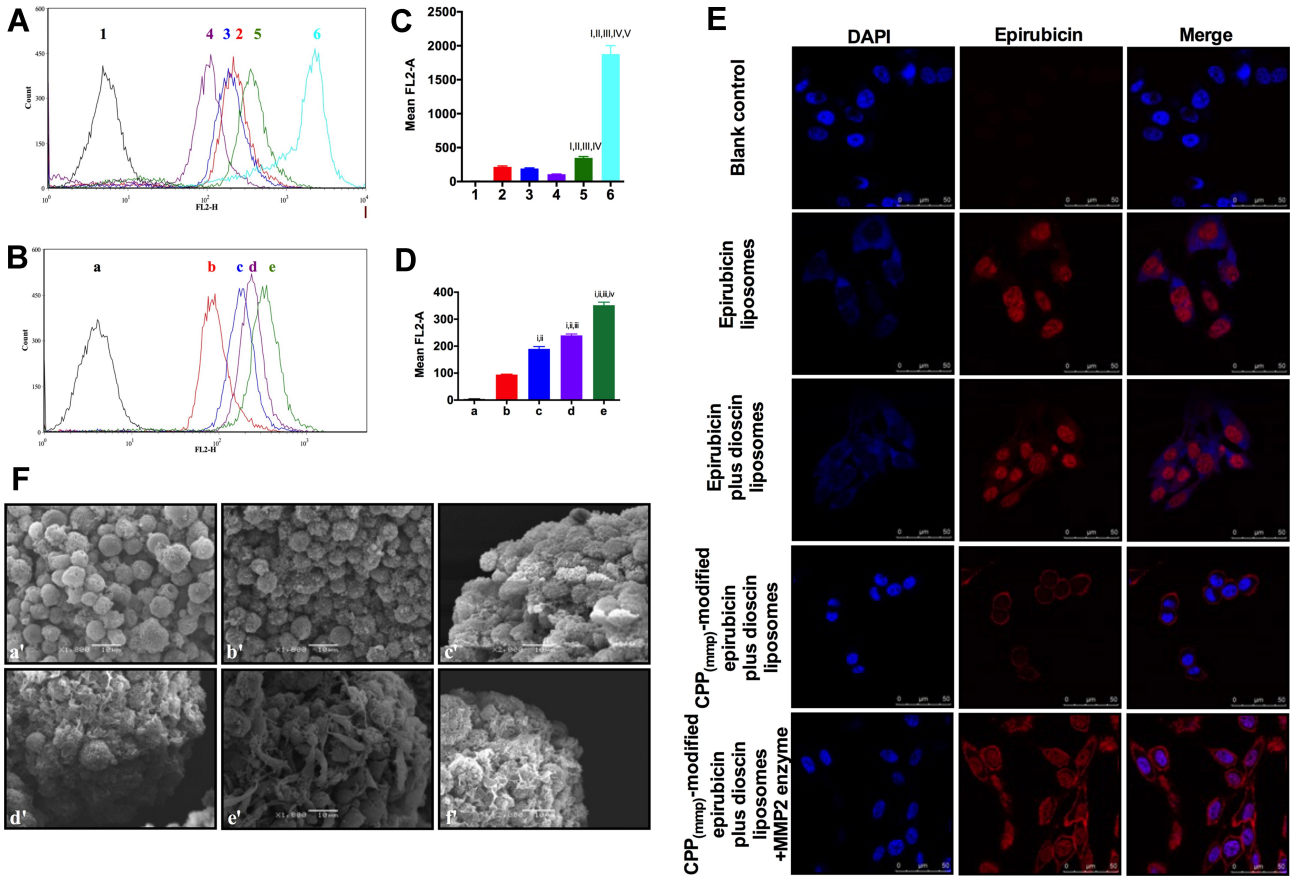

Figure 3 Cellular uptake and localization after incubation with varying formulations. (**A**) Cellular uptake of A549 cells treated with the varying liposomal formulations or free vinorelbine; (**B**) quantitative analysis of fluorescence intensity; 1. Blank control; 2. Epirubicin liposomes; 3. Epirubicin plus dioscin liposomes; 4. CPP $_{(mmp)}$ modified epirubicin plus dioscin liposomes; 5. CPP $_{(mmp)}$ modified epirubicin plus dioscin liposomes + MMP2 enzymes; 6. Free epirubicin; Data are presented as mean ± SD (n=3). I, vs 1; II, vs 2; III, vs 3; IV, vs 4; V, vs 5. $P<0.05$; (**C**) cellular uptake of A549 cells treated with CPP $_{(mmp)}$ modified epirubicin plus dioscin liposomes incubated with different concentrations of MMP2 enzymes; (**D**) quantitative analysis of fluorescence intensity; a. Blank control; b. CPP $_{(mmp)}$ modified epirubicin plus dioscin liposomes without MMP2 enzymes; c. CPP $_{(mmp)}$ modified epirubicin plus dioscin liposomes incubated with MMP2 enzymes (0.2 μM); d. CPP $_{(mmp)}$ modified epirubicin plus dioscin liposomes incubated with MMP2 enzymes (0.5 μM); e. CPP $_{(mmp)}$ modified epirubicin plus dioscin liposomes incubated with MMP2 enzymes (1 μM); Data are presented as mean ± SD (n=3). i, vs a; ii, vs b; iii, vs c; iv, vs d; $P<0.05$; (**E**) analysis of localization of A549 cells incubated with the varying formulations by laser scanning confocal microscopy, scale bar=100 μm (n=3). (**F**) SEM photographs of A549 spheroids. a'. Blank control; b'. Dioscin liposomes; c'. Vinorelbine liposomes; d'. Vinorelbine plus dioscin liposomes; e'. CPP $_{(mmp)}$ modified vinorelbine plus dioscin liposomes; f'. CPP $_{(mmp)}$ modified vinorelbine plus dioscin liposomes incubated with MMP2 enzymes.

enzymes > CPP $_{(mmp)}$ modified vinorelbine plus dioscin liposomes ≥ vinorelbine plus dioscin liposomes > vinorelbine liposomes > dioscin liposomes.

Cytotoxic Effects

The cytotoxicity of the varying free drug and liposomal formulations for A549 cells were measured by CCK-8 assay in Figure 4. Results showed that vinorelbine exhibited strong cytotoxicity against A549 cells. When the concentration of free vinorelbine was 0.1 μM, the survival rates of A549 cells were nearly 30%. Furthermore, the cytotoxic effect of free vinorelbine was further enhanced by the addition of different concentrations of dioscin with a concentration-dependent manner (molar ratios of 1:10, 1:20, and 1:50). At a 1:50 molar ratio between the drugs, the IC_{50} value was (0.0023 ± 0.002 μM), considerably lower than that of free vinorelbine (0.038 ± 0.002 μM) (Figure 4A). Figure 4B exhibits the inhibitory effects of varying liposomal formulations on A549 cells. Results showed that blank liposomes exhibited negligible cytotoxicity against A549 cells for 48 h, which indicated the good biocompatibility of nanocarriers, and dioscin liposomes showed little cytotoxicity within the range of 0–10 μM. For the varying liposomal formulations, the ranks of cytotoxicity to A549 cells were CPP $_{(mmp)}$ modified vinorelbine plus dioscin liposomes + MMP2 enzymes > CPP $_{(mmp)}$ modified vinorelbine plus dioscin liposomes ≥ vinorelbine plus dioscin liposomes > vinorelbine liposomes > dioscin liposomes. And the IC_{50} values for vinorelbine liposomes, vinorelbine plus dioscin liposomes, CPP $_{(mmp)}$ modified vinorelbine plus dioscin liposomes, and CPP $_{(mmp)}$ modified vinorelbine plus dioscin liposomes + MMP2 enzymes were 0.050 ± 0.011 μM,

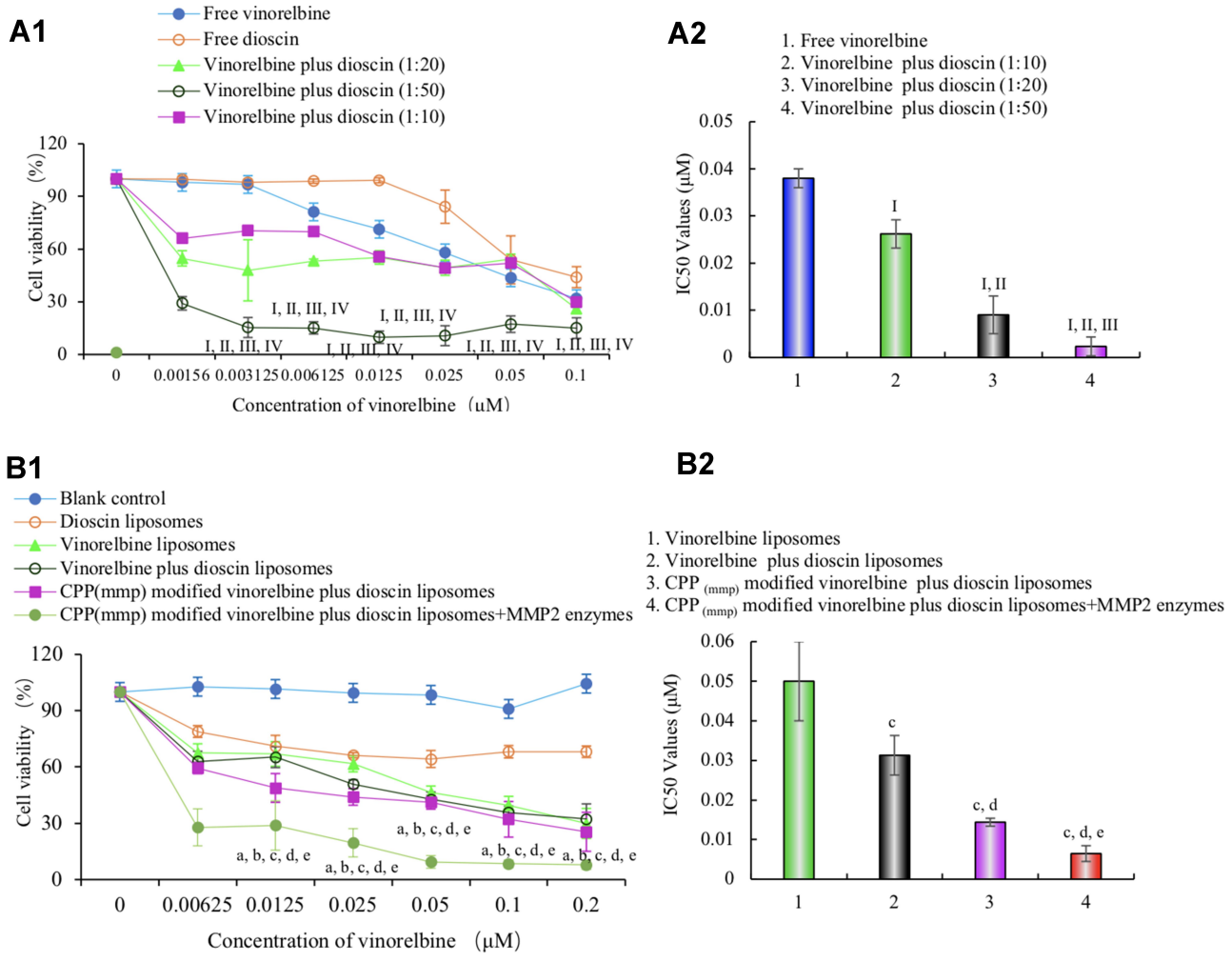

Figure 4 Cytotoxic effects on A549 cells after treatments with varying formulations. (**A**) Cytotoxic effects of free drugs; I, vs Free vinorelbine; II, vs Free dioscin; III, vs Free vinorelbine plus dioscin (1:10); IV, vs Free vinorelbine plus dioscin (1:20); (**B**) cytotoxic effects of the liposomal formulations. a, vs Blank control liposomes; b, vs Dioscin liposomes; c, vs Vinorelbine liposomes; d, vs Vinorelbine plus dioscin liposomes; e, vs CPP $_{(mmp)}$ modified vinorelbine plus dioscin liposomes. Data are presented as mean ±SD (n=6). $P<0.05$.

0.031 ± 0.005 μM, 0.014 ± 0.001 μM, and 0.006 ± 0.002 μM, respectively. Among all the liposomal formulations, CPP $_{(mmp)}$ modified vinorelbine plus dioscin liposomes + MMP2 enzymes showed the most obvious cytotoxicity on A549 cells. The phenomenon was due to the exposure of CPP on the liposomal surface after incubation with MMP2 enzymes.

Inhibition of Tumor Cells Invasion and Migration

Cell migration is a normal physiological process, required for chemotaxis of white blood cells and directional movement of cells from other tissues. However, in tumor tissue, the invasion and migration of malignant tumor cells are significantly associated with the likelihood of patient death. Usually, tumor cell invasion and migration mainly include a series of processes as follows: (i) during the early stages of metastasis, VM is formed by tumor cells to provide nutrition and a chance for subsequently invading to other site; (ii) tumor cells detach from the primary tumor sites and transfer into nearby tissues through the basement membrane; (iii) epigenetic tumor cells transform into mesenchymal cells (EMT), and the intercellular connections are loose, leading to decreased adhesion, enhanced migration and diffusion of tumor cells, and the formation of invasive tumor cells (iv) invasive tumor cells enter the blood vessels and survive in the blood circulation; (v) invasive tumor cells arrive at the metastatic site, colonize and grow at the new environment and form a metastatic tumor.[35,36] Invasion and metastasis are two barriers in treatment of NSCLC. Therefore, it is necessary to investigate whether drug-loaded liposomes could obviously inhibit tumor cell invasion and migration.[37] Results of the Transwell invasion assay are shown in Figure 5A and D. We found that the transmembrane migratory capability of A549 cells was inhibited to varying degrees following treatments with the varying liposomal formulations. Among all the groups, CPP $_{(mmp)}$ modified vinorelbine plus dioscin liposomes + MMP2 enzymes showed the strongest invasive inhibitory effect on A549 cell invasion.

Figure 5B shows the inhibitory of migration after treatments with the varying liposomal formulations. The wound-healing results suggested that all drug-loaded liposomal formulations inhibited the migration of A549 cells. A quantitative evaluation by ImageJ software analysis showed that the rank of relative migration inhibitory effect was: CPP $_{(mmp)}$ modified vinorelbine plus dioscin liposomes + MMP2 enzymes > vinorelbine plus dioscin liposomes > CPP $_{(mmp)}$ modified vinorelbine plus dioscin liposomes > dioscin liposomes > vinorelbine liposomes (Figure 5E). Dioscin is a natural product isolated from certain medicinal plants, such as *Dioscorea Nipponica* and *Paridis rhizome*. The potential anti-tumor effect of dioscin has been confirmed in various cancer cells including NSCLC A549 cells, which is shown to inhibit the invasion and metastasis of tumor cells.[38] Our previous research results also showed that the dioscin as a regulator encapsulated in liposomes can play an ideal anti-tumor effect, which is manifested as inhibition of tumor cell invasion and migration, anti-angiogenesis and VM formation.[19,23] Based on the above, we chose dioscin as a regulator, encapsulated inside the liposomes, and played a helpful anti-tumor effect in this study. Our results also indicated that the addition of dioscin could significantly inhibit the tumor cells' invasion and migration.

In addition, accumulating evidences have suggested that EMT is critical to the invasion and migration of cancer cells, during which cancer cells acquire the ability to invade and resist apoptosis.[39,40] Figure 5C denotes the inhibition of EMT processes by the varying liposomal formulations. Results showed that the cell morphology of the heated A549 cells was significantly different from that of the unheated cells. A549 cells under normal conditions were cuboidal with rounded edges, high intercellular fusion and a similar morphology. After being heated for 10 min, the cells' morphology changed to a long spindle shape and the degree of intercellular fusion was decreased. Results showed that the capacity of CPP $_{(mmp)}$ modified vinorelbine plus dioscin liposomes + MMP2 enzymes to suppress EMT of A549 cells was significantly stronger than that all of other liposomes (Figure 5F).

Inhibition of VM Formation in vitro

Vasculogenic mimicry (VM) was firstly reported in melanoma by Maniotis et al, and it had been identified in a variety of solid tumors, including NSCLC, ovarian cancer, breast cancer, glioma and liver cancer.[41] The existence of VM was associated with enhanced metastasis and reduced survival in cancer patients.[42] VM is the ability of invasive cancer cells to acquire altered phenotypes and to form the vascular system without relying on endothelial cells, and it is an entirely new model of tumor blood supply. In the VM, vascular channels consist of periodic acid-schiff (PAS)-positive basement membrane and CD31-negative epithelial colorectal cell.[43] These vessels allow

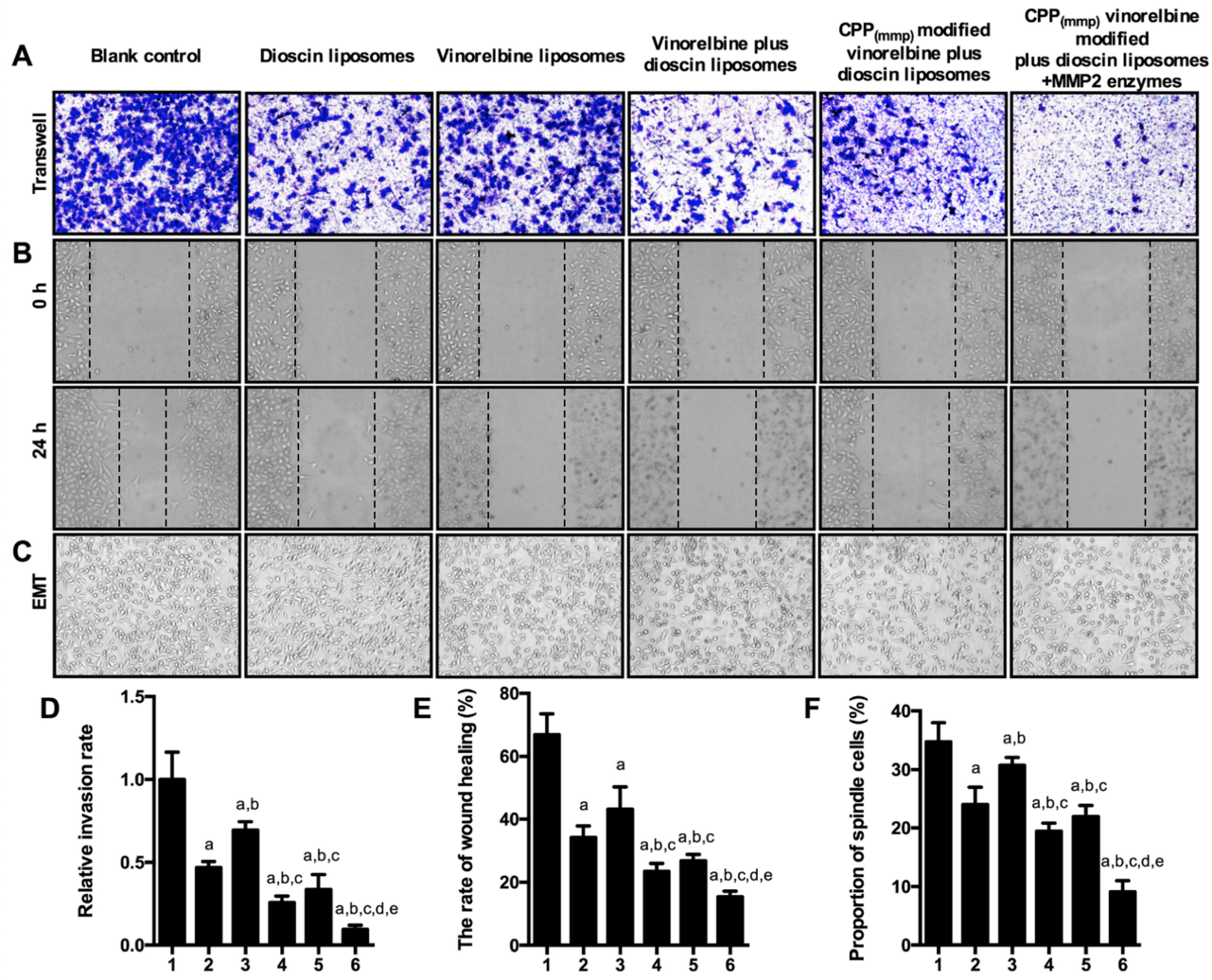

Figure 5 Inhibitory effects on invasion, migration and EMT in A549 cells after treatment with varying liposomal formulations. (**A**) Representative images of A549 cells invasion after treatment with the varying liposomal formulations, scale bar=50 μm; (**B**) representative images of A549 cells wound closure following treatment with the varying liposomal formulations after 24 h, scale bar=50 μm; (**C**) representative images of inhibition of A549 cells EMT by the varying liposomal formulations, scale bar=50 μm; (**D**) semi-quantitative analysis of relative invasion rate of A549 cells after treatment with the varying liposomal formulations. Data are presented as mean±SD (n=6); (**E**) quantitative analysis of wound-healing rate of A549 cells after treatment with the varying liposomal formulations. Data are presented as mean±SD (n=6); (**F**) quantitative analysis of spindle cells proportion of A549 cells after treatment with the varying liposomal formulations. Data are presented as mean±SD (n=6). 1. Blank control; 2. Dioscin liposomes; 3. Vinorelbine liposomes; 4. Vinorelbine plus dioscin liposomes; 5. CPP $_{(mmp)}$ modified vinorelbine plus dioscin liposomes; 6. CPP $_{(mmp)}$ modified vinorelbine plus dioscin liposomes incubated with MMP2 enzymes; a, vs 1; b, vs 2; c, vs 3; d, vs 4; e, vs 5; $P<0.05$.

red blood cells to pass through, exposing tumor cells directly to the blood supply and greatly increasing the probability of metastasis. The mechanism of VM generation was associated with hypoxia, which may promote the transmit phenotypes of tumor cells with VM capability.[44] In this study, Figure 6 depicts the destructive effects on VM channels after treatments with the varying liposomal formulations. We found that vascular-like structures were observed near A549 cells on the Matrigel in the blank control group. However, dioscin-loaded liposomal formulations exhibited obvious destructive effects on VM channels. Among all the liposomal formulations, CPP $_{(mmp)}$ modified vinorelbine plus dioscin liposomes + MMP2 enzymes exhibited the strongest inhibitory effect on VM (Figure 6A and B).

Inhibition of Angiogenesis

More and more studies suggest that angiogenesis is one of the hallmarks of malignant cancer.[45] When the tumors grow to a certain size, they need angiogenesis to maintain their nutritional supply for sustainable development. Angiogenesis has been identified as a complex process, such as the degradation of the basement membrane near the original vessels and endothelial cell (EC) proliferation,

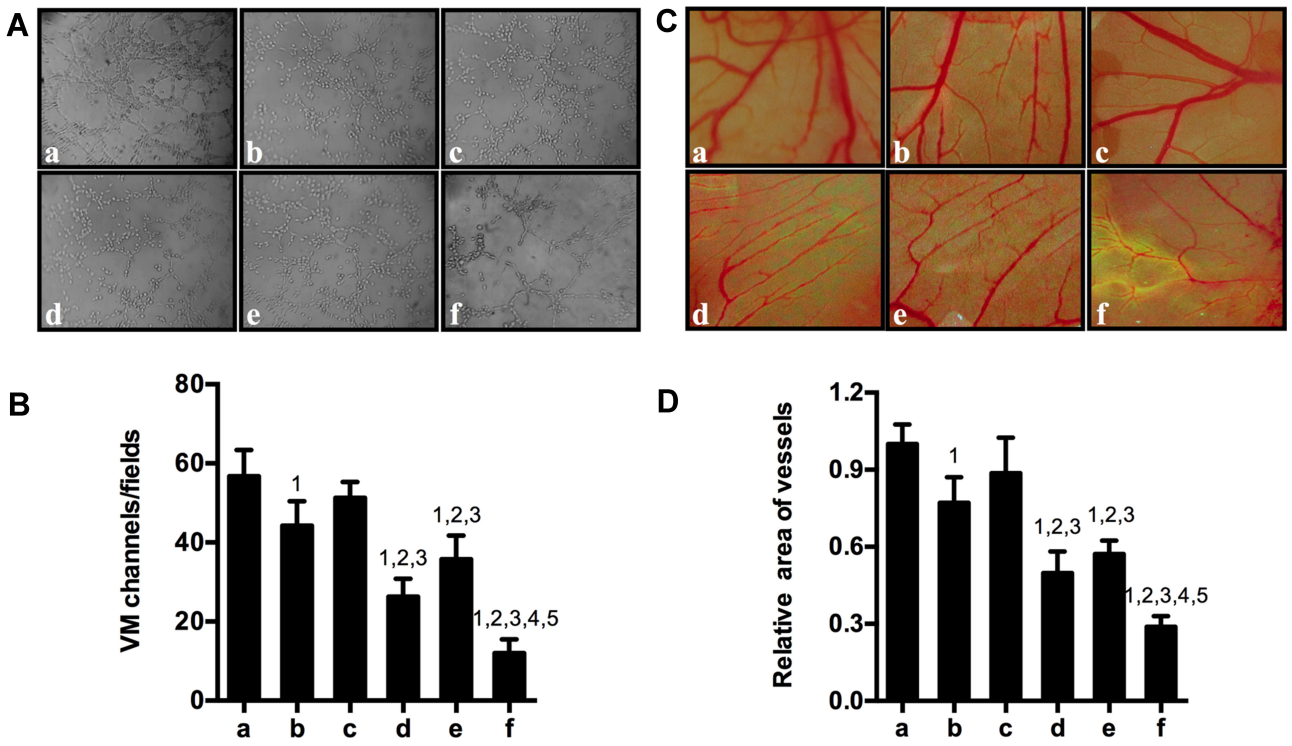

Figure 6 Inhibitory effects on VM channels formation and angiogenesis after treatment with varying liposomal formulations. (**A**) Inhibition of VM channels formation in vitro, scale bar=50 μm; (**B**) quantitative analysis of the number of VM channels; (**C**) inhibition of angiogenesis on CAM after treatment with the varying liposomal formulations, scale bar=5 mm; (**D**) analysis of relative area vessels after treatment with the varying liposomal formulations. Data are presented as mean±SD (n=6). a. Blank control; b. Dioscin liposomes; c. Vinorelbine liposomes; d. Vinorelbine plus dioscin liposomes; e. CPP $_{(mmp)}$ modified vinorelbine plus dioscin liposomes; f. CPP $_{(mmp)}$ modified vinorelbine plus dioscin liposomes incubated with MMP2 enzymes; 1, vs a; 2, vs b; 3, vs c; 4, vs d; 5, vs e. $P<0.05$.

migration, aggregation and new tube formation, resulting in the formation of a new vascular system.[46] To date, anti-angiogenic therapy has become to be one of the antitumor strategies. A considerable number of anti-angiogenic drugs have been approved by the US Food and Drug Administration (FDA) and have been used in cancer treatment. However, the antitumor effect of antiangiogenic therapy alone is not ideal.[47] In this study, the chorioallantoic membrane (CAM) assay was used to evaluate the antiangiogenic effect after treatments with the various liposomal formulations (Figure 6C and D). Results showed that the blood vessels grew vigorously and the density of new vessels increased in blank control group. In contrast, new vessels' density was significantly decreased after treatment with the various liposomal formulations, and CPP $_{(mmp)}$ modified vinorelbine plus dioscin liposomes + MMP2 enzymes showed the strongest inhibitory effect on CAM angiogenesis. The results showed that CPP $_{(mmp)}$ modified vinorelbine plus dioscin liposomes + MMP2 enzymes had the effect of inhibiting the VM channels and angiogenesis, thereby limiting the nutrient supply required for tumor cell proliferation, invasion and migration.

Fluorescence Imaging in vivo

To validate the tumor-targeting and tumor-penetrating ability of the varying formulations, the in vivo and ex vivo imaging was used. Figure 7A presents the real-time distribution and accumulation ability of the varying formulations in tumor-bearing nude mice. The fluorescence signal of CPP $_{(mmp)}$ modified DiR plus dioscin liposomes exhibited the strongest tumor accumulation in the tumor sites and maintained for up to 48 h. In contrast, free DiR was mainly distributed in the liver and gradually weakened or disappeared after 24 h. Figure 7B illustrates the ex vivo optical images of tumor masses and major organs after the tumor-bearing mice were sacrificed at 48 h. Results exhibited that the fluorescence of the CPP $_{(mmp)}$ modified DiR plus dioscin liposomes was still observed in tumor masses and in major organs (liver and spleen). In contrast, the fluorescence signal was invisible in tumor masses after injection of free DiR. The prolonged circulation time and enhanced accumulation in tumor sites could be explained by the modification of CPP-PVGLIG-PEG$_{5000}$ on the liposomal surface. On the one hand, according to Figure 1A, the hydrophilic PEG$_{5000}$ formed a hydration film on the liposomal surface to protect

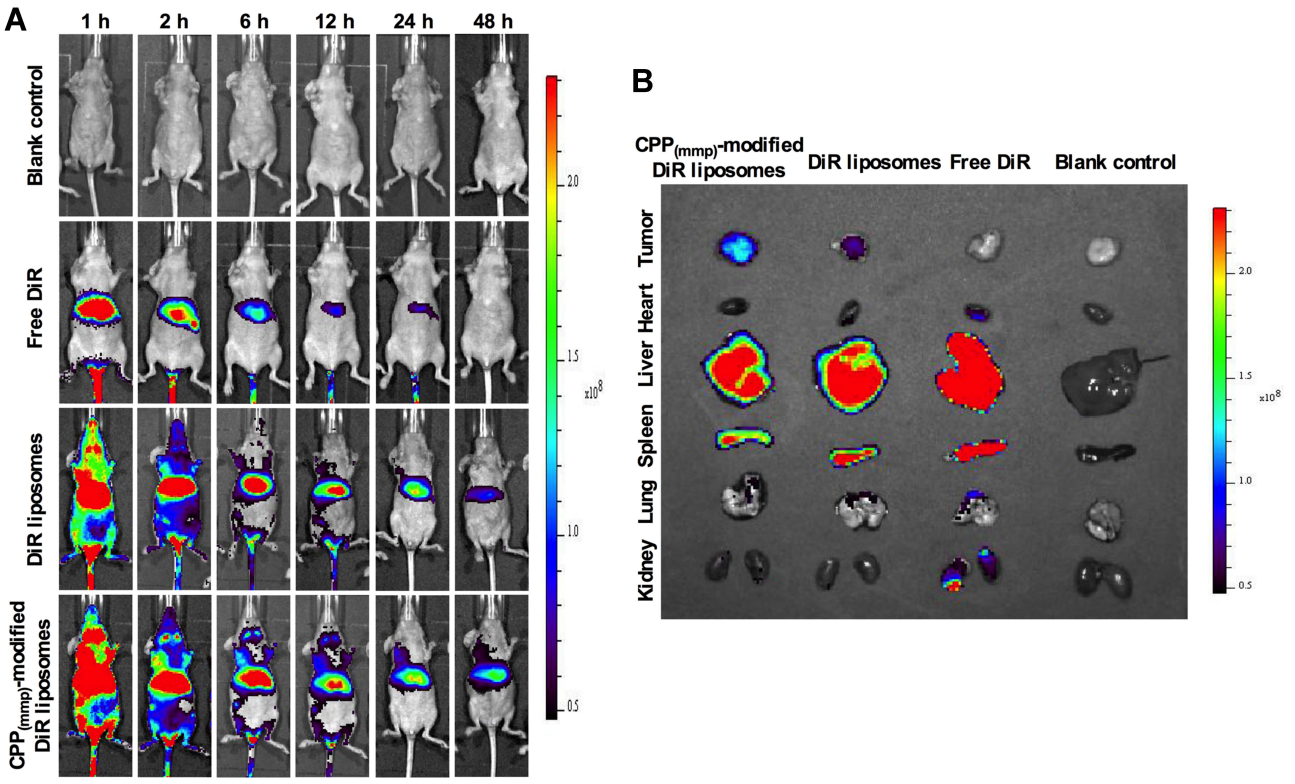

Figure 7 Real-time imaging observation after intravenous administration of varying liposomal formulations in tumor-bearing mice. (**A**) Real-time images in vivo; (**B**) ex vivo optical images of tumor tissues, heart, liver, spleen, lung, and kidney at 48 h (n=3).

the positively charged CPP and liposomes. On the other, the enzyme-sensitive molecule PVGLIG on the outermost side of liposomes will be hydrolyzed by the overexpressed MMP2 enzymes in tumor microenvironment, thus exposing the targeting molecule CPP to enhance active targeting via electrostatic adsorption.[16,48]

Antitumor Efficacy in Tumor-Bearing Mice

Figure 8 shows the pharmacodynamics after treatments with the varying formulations. Compared with the blank control group, all drug-treated groups showed different degrees of tumor growth inhibition (Figure 8A). Among all the liposomal formulations, CPP $_{(mmp)}$ modified vinorelbine plus dioscin liposomes showed the most significant tumor growth inhibitory effect on tumor volume from the 4th day after the start of administration, and the mice body weight was no significant decreased after treatments with the varying liposomal formulations, indicating that all the liposomal formulations had ideal biocompatibility (Figure 8B). In addition, administration of the CPP$_{(mmp)}$ modified vinorelbine plus dioscin liposomes resulted in hematological parameters similar to the saline-treated group, indicating that the CPP$_{(mmp)}$ modified liposomes are safe and non-toxic (Results not shown).

H&E staining of tumor tissue sections showed that CPP $_{(mmp)}$ modified vinorelbine plus dioscin liposomes significantly increased necrotic cells and disrupted the structure of tumor tissues (Figure 8C). Moreover, to detect apoptotic and proliferative cells in tumor tissues, TUNEL assay and Ki67-antibody staining were performed, respectively. As shown in Figure 8C–E, results showed that almost no apoptotic cell was in the blank control group. However, the number of apoptotic cells increased after treatment with CPP $_{(mmp)}$ modified vinorelbine plus dioscin liposomes. According to the results from TUNEL assay, the rank of the number of apoptotic cells was as follows: CPP $_{(mmp)}$ modified vinorelbine plus dioscin liposomes > vinorelbine plus dioscin liposomes > vinorelbine liposomes > free vinorelbine > blank control. Furthermore, the number of Ki67-positive cells significantly reduced after treatment with CPP $_{(mmp)}$ modified vinorelbine plus dioscin liposomes, which was opposite to the trend of apoptosis detected by TUNEL assay.

To assess the inhibitory effects on VM formation after treatments with the varying formulations in vivo, tumor

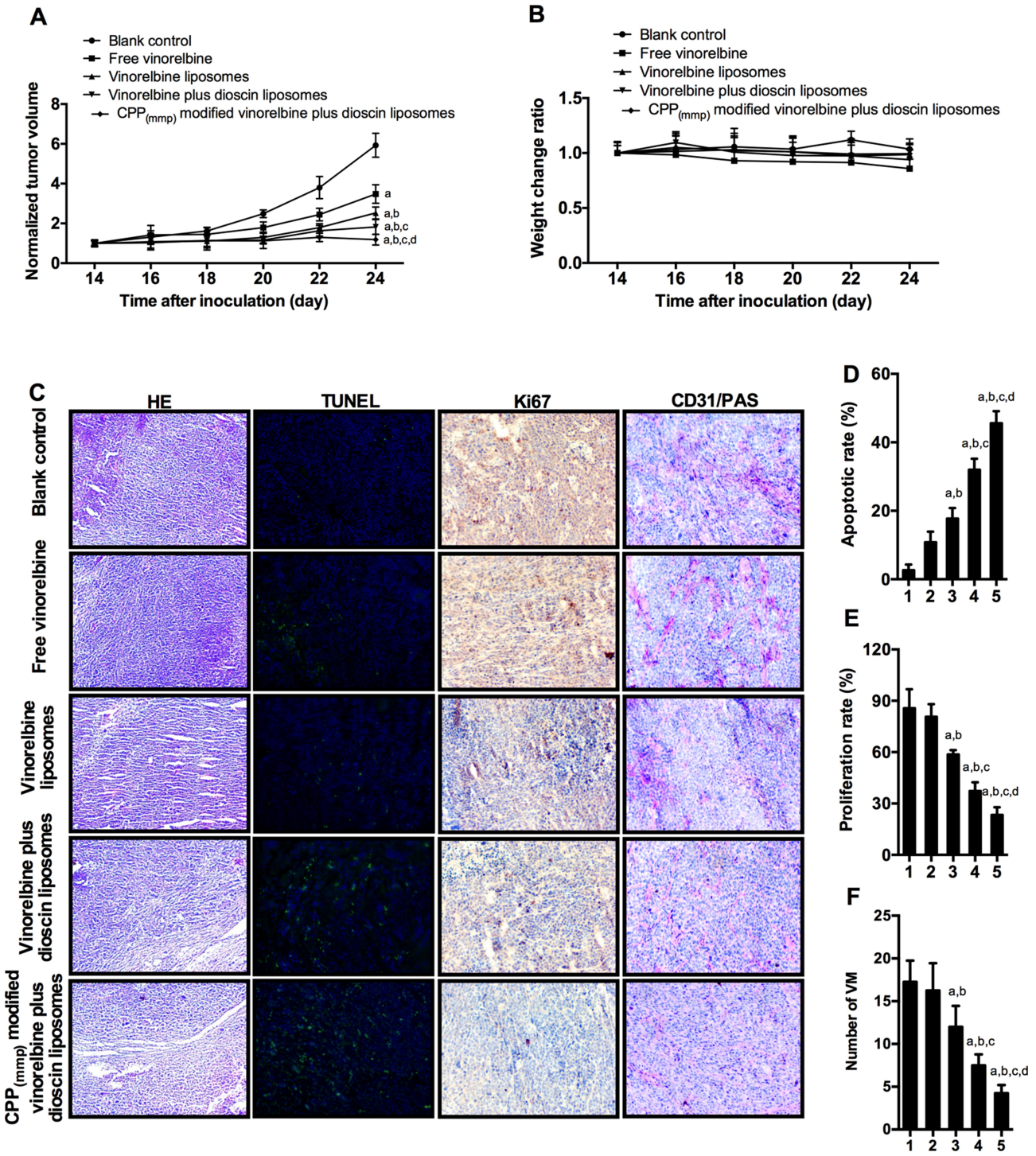

Figure 8 Antitumor efficacy after treatment with the varying formulations in vivo. (**A**) Tumor volume changes ratio was analysis during the treatment process; (**B**) body weight changes ratio was analysis during the treatment process; (**C**) representative images of HE staining, TUNEL assay, Ki67-antibody staining and CD31/PAS staining, scalar bar=50 μm; (**D**) quantitative analysis of apoptotic rate; (**E**) quantitative analysis of proliferation rate; (**F**) quantitative analysis of the number of VM channels in each group. Data are presented as mean±SD (n=6). 1. Blank control; 2. Free vinorelbine; 3. Vinorelbine liposomes; 4. Vinorelbine plus dioscin liposomes; 5. CPP $_{(mmp)}$ modified vinorelbine plus dioscin liposomes. a, vs 1; b, vs 2; c, vs 3; d, vs 4. $P<0.05$.

tissue sections were stained with CD31/PAS double staining. Results showed CD31-negative and PAS-positive channels formed in tumor tissues after treatment with blank control group, thereby revealing NSCLC VM channels formation. In contrast, fewer VM channels were observed after treatment with CPP $_{(mmp)}$ modified vinorelbine plus dioscin liposomes, suggesting the obvious inhibitory effect on VM formations (Figure 8C and F).

From the above results, CPP $_{(mmp)}$ modified vinorelbine plus dioscin liposomes exhibited the strongest inhibitory effect on VM formation in vivo.

Based on current data, we suggest the following events describe the behavior of the targeting delivery system in vivo. After intravenous administration, CPP $_{(mmp)}$ modified vinorelbine plus dioscin liposomes exhibited prolonged blood circulation time, which was in favor of being accumulated in tumor sites by EPR effect. After accumulation in tumor sites, the MMP2 enzymes overexpressed in tumor microenvironment will cleave the MMP2-sensitive peptide linker in the liposomal surface. The breaking of the linker caused the elimination of hydrophilic PEG_{5000} and exposed the positively charged CPP on the liposomal surface, which enhanced cellular internalization of antitumor drugs by tumor cells via electrostatic adsorption. Therefore, the novel multifunctional liposomes responding to overexpressed MMP2 enzyme should provide a potential treatment strategy for NSCLC.

Conclusion

In conclusion, we had demonstrated that CPP $_{(mmp)}$ modified vinorelbine plus dioscin liposomes could enhance antitumor efficacy in vitro and in vivo. As a kind of multifunctional liposomal drug carrier, it had the following advantages: (i) the high encapsulation efficiencies and ideal particle size of the liposomes are conducive to their enrichment in tumor sites through passive targeting effects; (ii) the hydrophilic PEG_{5000} formed a hydration film on the liposomal surface to protect the positively charged CPP, which prevented non-specific intracellular uptake of CPP; (iii) the MMP2 cleavable linker between the hydrophilic PEG_{5000} and the nanocarrier could be cleaved and exposed the positively charged CPP, which enhanced the active targeting via electrostatic adsorption; (iv) dioscin encapsulated in the liposomes enhanced the anti-tumor efficacy by inhibiting VM channel formation, angiogenesis, migration and invasion. Therefore, CPP (mmp) modified vinorelbine plus dioscin liposomes offer a potential strategy for treating NSCLC.

Acknowledgments

This work was supported by the National Natural Science Foundation of China (No. 81874347 and 81703453), Liaoning Revitalization Talents Program (Grant No. XLYC1807132) and Liaoning Natural Science Foundation (Grant No. 2019-MS-226).

Disclosure

All authors declare that there are no conflicts of interest.

References

1. Chan AWH, Tong JHM, Kwan JSH, et al. Assessment of programmed cell death ligand-1 expression by 4 diagnostic assays and its clinicopathological correlation in a large cohort of surgical resected non-small cell lung carcinoma. *Mod Pathol*. 2018;31:1381–1390. doi:10.1038/s41379-018-0053-3
2. Jiang J, Xu Y, Ren H, et al. MKRN2 inhibits migration and invasion of non-small-cell lung cancer by negatively regulating the PI3K/Akt pathway. *J Exp Clin Cancer Res*. 2018;37:189. doi:10.1186/s13046-018-0855-7
3. Wu T, Hu H, Zhang T, et al. miR-25 promotes cell proliferation, migration, and invasion of non-small-cell lung cancer by targeting the LATS2/YAP signaling pathway. *Oxid Med Cell Longev*. 2019;2019:1–14. doi:10.1155/2019/3832648
4. Jiang R, Hu C, Li Q, et al. Sodium new houttuyfonate suppresses metastasis in NSCLC cells through the Linc00668/miR-147a/slug axis. *J Exp Clin Cancer Res*. 2019;38(1):155. doi:10.1186/s13046-019-1152-9
5. Li F, Wang Y, Chen W-L, et al. Co-delivery of VEGF siRNA and etoposide for enhanced anti-angiogenesis and anti-proliferation effect via multi-functional nanoparticles for orthotopic non-small cell lung cancer treatment. *Theranostics*. 2019;9:5886–5898. doi:10.7150/thno.32416
6. Adam LC, Raja J, Ludwig JM, Adeniran A, Gettinger SN, Kim HS. Cryotherapy for nodal metastasis in NSCLC with acquired resistance to immunotherapy. *J Immunother Cancer*. 2018;6. doi:10.1186/s40425-018-0468-x
7. Rocco D, Della Gravara L, Battiloro C, Gridelli C. The role of combination chemo-immunotherapy in advanced non-small cell lung cancer. *Expert Rev Anticancer Ther*. 2019;19(7):561–568. doi:10.1080/14737140.2019.1631800
8. Shafique M, Tanvetyanon T. Immunotherapy alone or chemo-immunotherapy as front-line treatment for advanced non-small cell lung cancer. *Expert Opin Biol Ther*. 2019;19(3):225–232. doi:10.1080/14712598.2019.1571036
9. Ramasamy T, Ruttala HB, Gupta B, et al. Smart chemistry-based nanosized drug delivery systems for systemic applications: a comprehensive review. *J Control Release*. 2017;258:226–253. doi:10.1016/j.jconrel.2017.04.043
10. Gupta B, Ramasamy T, Poudel BK, et al. Development of bioactive PEGylated nanostructured platforms for sequential delivery of doxorubicin and imatinib to overcome drug resistance in metastatic tumors. *ACS Appl Mater Interfaces*. 2017;9(11):9280–9290. doi:10.1021/acsami.6b09163
11. Li M, Song W, Tang Z, et al. Nanoscaled poly(L-glutamic acid)/doxorubicin-amphiphile complex as pH-responsive drug delivery system for effective treatment of nonsmall cell lung cancer. *ACS Appl Mater Interfaces*. 2013;5:1781–1792. doi:10.1021/am303073u
12. Koren E, Torchilin VP. Cell-penetrating peptides: breaking through to the other side. *Trends Mol Med*. 2012;18(7):385–393. doi:10.1016/j.molmed.2012.04.012
13. Ramasamy T, Ruttala HB, Chitrapriya N, et al. Engineering of cell microenvironment-responsive polypeptide nanovehicle co-encapsulating a synergistic combination of small molecules for effective chemotherapy in solid tumors. *Acta Biomater*. 2017;48:131–143. doi:10.1016/j.actbio.2016.10.034
14. Takeoka S, Li T. A novel application of maleimide for advanced drug delivery: in vitro and in vivo evaluation of maleimide-modified pH-sensitive liposomes. *Int J Nanomedicine*. 2013;3855. doi:10.2147/IJN.S47749

15. Chen B, Dai W, He B, et al. Current multistage drug delivery systems based on the tumor microenvironment. *Theranostics*. 2017;7:538–558. doi:10.7150/thno.16684
16. Zhu L, Kate P, Torchilin VP. Matrix metalloprotease 2-responsive multifunctional liposomal nanocarrier for enhanced tumor targeting. *ACS Nano*. 2012;6(4):3491–3498. doi:10.1021/nn300524f
17. Cun X, Chen J, Ruan S, et al. A novel strategy through combining iRGD peptide with tumor-microenvironment-responsive and multi-stage nanoparticles for deep tumor penetration. *ACS Appl Mater Interfaces*. 2015;7:27458–27466. doi:10.1021/acsami.5b09391
18. Ji T, Li S, Zhang Y, et al. An MMP-2 responsive liposome integrating antifibrosis and chemotherapeutic drugs for enhanced drug perfusion and efficacy in pancreatic cancer. *ACS Appl Mater Interfaces*. 2016;8:3438–3445. doi:10.1021/acsami.5b11619
19. Kong L, Cai F, Yao X, et al. RPV-modified epirubicin and dioscin co-delivery liposomes suppress non-small cell lung cancer growth by limiting nutrition supply. *Cancer Sci*. 2020;111:621–636. doi:10.1111/cas.14256
20. Wan Y, Han J, Fan G, Zhang Z, Gong T, Sun X. Enzyme-responsive liposomes modified adenoviral vectors for enhanced tumor cell transduction and reduced immunogenicity. *Biomaterials*. 2013;34:3020–3030. doi:10.1016/j.biomaterials.2012.12.051
21. Ju RJ, Li XT, Shi JF, et al. Liposomes, modified with PTD(HIV-1) peptide, containing epirubicin and celecoxib, to target vasculogenic mimicry channels in invasive breast cancer. *Biomaterials*. 2014;35:7610–7621. doi:10.1016/j.biomaterials.2014.05.040
22. Ramasamy T, Ruttala HB, Kaliraj K, et al. Polypeptide derivative of metformin with the combined advantage of a gene carrier and anticancer activity. *ACS Biomater Sci Eng*. 2019;5:5159–5168. doi:10.1021/acsbiomaterials.9b00982
23. Wang Y, Fu M, Liu J, et al. Inhibition of tumor metastasis by targeted daunorubicin and dioscin codelivery liposomes modified with PFV for the treatment of non-small-cell lung cancer. *Int J Nanomedicine*. 2019;14:4071–4090. doi:10.2147/IJN.S194304
24. Lin C, Zhang X, Chen H, et al. Dual-ligand modified liposomes provide effective local targeted delivery of lung-cancer drug by antibody and tumor lineage-homing cell-penetrating peptide. *Drug Deliv*. 2018;25:256–266. doi:10.1080/10717544.2018.1425777
25. Xie X, Shao X, Ma W, et al. Overcoming drug-resistant lung cancer by paclitaxel loaded tetrahedral DNA nanostructures. *Nanoscale*. 2018;10(12):5457–5465. doi:10.1039/C7NR09692E
26. Azad T, Janse van Rensburg HJ, Lightbody ED, et al. A LATS biosensor screen identifies VEGFR as a regulator of the Hippo pathway in angiogenesis. *Nat Commun*. 2018;9. doi:10.1038/s41467-018-03278-w
27. Zhuge Y, Regueiro MM, Tian R, et al. The effect of estrogen on diabetic wound healing is mediated through increasing the function of various bone marrow-derived progenitor cells. *J Vasc Surg*. 2018;68:1–9. doi:10.1016/j.jvs.2018.04.069
28. Cirligeriu L, Cimpean AM, Calniceanu H, et al. Hyaluronic acid/bone substitute complex implanted on chick embryo chorioallantoic membrane induces osteoblastic differentiation and angiogenesis, but not inflammation. *Int J Mol Sci*. 2018;19:4119. doi:10.3390/ijms19124119
29. Zhang J, Xu Z, Dai H, Zhao J, Liu T, Zhang G. Silencing of forkhead box M1 reverses transforming growth factor-β1-induced invasion and epithelial-mesenchymal transition of endometriotic epithelial cells. *Gynecol Obstet Invest*. 2019;84:485–494. doi:10.1159/000499625
30. Zhu L, Wang T, Perche F, Taigind A, Torchilin VP. Enhanced anticancer activity of nanopreparation containing an MMP2-sensitive PEG-drug conjugate and cell-penetrating moiety. *Proc Natl Acad Sci U S A*. 2013;110(42):17047–17052. doi:10.1073/pnas.1304987110
31. Liu J, Zhang B, Luo Z, et al. Enzyme responsive mesoporous silica nanoparticles for targeted tumor therapy in vitro and in vivo. *Nanoscale*. 2015;7(8):3614–3626. doi:10.1039/C5NR00072F
32. Chen W-H, Luo G-F, Lei Q, et al. MMP-2 responsive polymeric micelles for cancer-targeted intracellular drug delivery. *Chem Commun*. 2015;51:465–468. doi:10.1039/C4CC07563C
33. Luo C, Miao L, Zhao Y, et al. A novel cationic lipid with intrinsic antitumor activity to facilitate gene therapy of TRAIL DNA. *Biomaterials*. 2016;102:239–248. doi:10.1016/j.biomaterials.2016.06.030
34. Li F, Mei H, Gao Y, et al. Co-delivery of oxygen and erlotinib by aptamer-modified liposomal complexes to reverse hypoxia-induced drug resistance in lung cancer. *Biomaterials*. 2017;145:56–71. doi:10.1016/j.biomaterials.2017.08.030
35. Xia R, Xu G, Huang Y, Sheng X, Xu X, Lu H. Hesperidin suppresses the migration and invasion of non-small cell lung cancer cells by inhibiting the SDF-1/CXCR-4 pathway. *Life Sci*. 2018;201:111–120. doi:10.1016/j.lfs.2018.03.046
36. Zhang D, Feng F, Li Q, Wang X, Yao L. Nanopurpurin-based photodynamic therapy destructs extracellular matrix against intractable tumor metastasis. *Biomaterials*. 2018;173:22–33. doi:10.1016/j.biomaterials.2018.04.045
37. Liang R, Xie J, Li J, et al. Liposomes-coated gold nanocages with antigens and adjuvants targeted delivery to dendritic cells for enhancing antitumor immune response. *Biomaterials*. 2017;149:41–50. doi:10.1016/j.biomaterials.2017.09.029
38. Lim WC, Kim H, Kim YJ, et al. Dioscin suppresses TGF-beta1-induced epithelial-mesenchymal transition and suppresses A549 lung cancer migration and invasion. *Bioorg Med Chem Lett*. 2017;27:3342–3348. doi:10.1016/j.bmcl.2017.06.014
39. Yoshida S, Kornek M, Ikenaga N, et al. Sublethal heat treatment promotes epithelial-mesenchymal transition and enhances the malignant potential of hepatocellular carcinoma. *Hepatology*. 2013;58:1667–1680. doi:10.1002/hep.26526
40. Watson KD, Lai CY, Qin S, et al. Ultrasound increases nanoparticle delivery by reducing intratumoral pressure and increasing transport in epithelial and epithelial-mesenchymal transition tumors. *Cancer Res*. 2012;72:1485–1493. doi:10.1158/0008-5472.CAN-11-3232
41. Maniotis AJ, Folberg R, Hess A, Seftor EA, Gardner LM, Pe'er J, et al. Vascular channel formation by human melanoma cells in vivo and in vitro: vasculogenic mimicry. *American Journal of Pathology*. 1999;155:739–752.
42. Stenzel M, Tura A, Nassar K, et al. Analysis of caveolin-1 and phosphoinositol-3 kinase expression in primary uveal melanomas. *Clin Experiment Ophthalmol*. 2016;44:400–409. doi:10.1111/ceo.12686
43. Yao L, Zhang D, Zhao X, et al. Dickkopf-1-promoted vasculogenic mimicry in non-small cell lung cancer is associated with EMT and development of a cancer stem-like cell phenotype. *J Cell Mol Med*. 2016;20:1673–1685. doi:10.1111/jcmm.12862
44. Wang M, Zhao X, Zhu D, et al. HIF-1alpha promoted vasculogenic mimicry formation in hepatocellular carcinoma through LOXL2 up-regulation in hypoxic tumor microenvironment. *J Exp Clin Cancer Res*. 2017;36:60. doi:10.1186/s13046-017-0533-1
45. Mao G, Liu Y, Fang X, et al. Tumor-derived microRNA-494 promotes angiogenesis in non-small cell lung cancer. *Angiogenesis*. 2015;18:373–382. doi:10.1007/s10456-015-9474-5
46. Lammers PE, Horn L. Targeting angiogenesis in advanced non-small cell lung cancer. *J Natl Compr Canc Netw*. 2013;11(10):1235–1247. doi:10.6004/jnccn.2013.0146
47. Itatani Y, Kawada K, Yamamoto T, Sakai Y. Resistance to anti-angiogenic therapy in cancer—alterations to anti-VEGF pathway. *Int J Mol Sci*. 2018;19:1232. doi:10.3390/ijms19041232
48. Ji T, Lang J, Wang J, et al. Designing liposomes to suppress extracellular matrix expression to enhance drug penetration and pancreatic tumor therapy. *ACS Nano*. 2017;11:8668–8678. doi:10.1021/acsnano.7b01026